

# Cerebellar-inspired bi-hemispheric neural network for adaptive control of an unstable robot

Ruben-Dario Pinzon-Morales, *Member, IEEE*, Yutaka Hirata, *Member, IEEE*

**Abstract**—In this paper, a cerebellar-inspired adaptive motor controller is constructed, and applied for adaptive control of a two-wheel balancing robot as an example. The controller comprises a feedback proportional and derivative (PD) controller and a realistic bi-hemispheric cerebellar neural network. The cerebellar network was configured based upon current anatomical and physiological knowledge of the cerebellar cortex, consisting of 1560 granular cells (Gr), 10 Golgi cells (Go), 10 basket/stellate cells (Ba/St), and two Purkinje cells (Pk). The network connectivity follows realistic synaptic converge and divergence ratios as close as possible within the limitation in the number of neuron models for real time execution. Each cell is described by a typical artificial neuron model whose output is a weighted sum of the inputs after a sigmoidal nonlinear transformation. The PD controller represents the non-cerebellar component working in tandem with the cerebellum in the brain. In the proposed controller, it provides the error signal for the cerebellar neural network to induce synaptic plasticity at the Gr-Pk synapses as in the real cerebellum. We demonstrate that the proposed cerebellar-inspired controller not only successfully control the balancing robot but also compensates for abrupt asymmetrical perturbations, which neither a PD controller alone nor a cerebellar network with a single hemispheric structure can cope with.

## I. INTRODUCTION

Reproduction of biological motor performance is a very difficult task due not only to the lack of equivalent energy efficient actuators but also to their highly evolved adaptabilities. In the brain, one of the structures related with such fine and precise adaptive motor control is the cerebellum. The cerebellum with its regular microcircuit structure extending all over its volume, and its learning capabilities is able to generate adequate commands for complex coordinated movements such as arm reaching, and the vestibuloocular reflex [1]. In robotics, initial attempts has been made to incorporate such neural circuitry into real world applications [2], [3].

In our previous work a single hemisphere cerebellar neuronal network controller was configured [3], and successfully tested in real world control of an unstable plant, namely, a two-wheel balancing robot. It was shown that the controller can manage abrupt perturbations imposed by loading the robot with an external weight located right above the robot (balanced load) that a PD controller alone cannot compensate for. However, when the external load was located off-centered either at the front or back of the robot, causing a major asymmetry in the forward and backward motion of the robot, the controller failed to continue stable control. In this study, an update of the single-hemisphere controller is made to

overcome previous limitations. We incorporate the bilateral structure of the cerebellum that is regarded crucial for the vestibuloocular reflex (VOR) motor learning [4], and other areas [5]. We also increase the number of neuron models so that realistic synaptic convergence and divergence ratios are maintained as close as possible within the limitation for real time execution of the controller. To test the validity of the new controller the two-wheel balancing robot is employed and an unbalanced load is imposed off-centered on the robot to affect its dynamics on the forward and backward movements asymmetrically.

This paper is organized as follow: in Sec. II a detailed description of the architecture of the proposed controller and the learning rule governing the network adaptability is introduced. In Sec. III the performance of the proposed controller is evaluated by considering two cases of perturbation: the balanced load placed on-centered the robot, and the unbalanced-asymmetrical load placed off-centered. Lastly, in Sec. IV discussion and conclusions are presented.

## II. METHODS

### A. Structure of the proposed controller

The proposed controller comprises a bi-hemisphere cerebellar neural network and a PD controller (Fig. 1). The PD controller assists the cerebellar controller while in the learning process. Therefore, the parameters of the PD controller ( $K_p$  and  $K_d$ ) were designed so that the PD controller alone can initially balance the robot without any load imposition. The cerebellar network structure was configured accordingly to the well-defined microcircuit of the cerebellum (Fig. 2), which has been extensively studied [6]. Among those cell types found so far in the cerebellar cortex, the following cells were incorporated, as their physiological and anatomical properties are well understood: Gr cells, Go cells, Ba/St cells, and Pk cell. Inputs to the cerebellum are conveyed via mossy fibers (mf). In the cerebellar flocculus that is involved in the VOR motor learning [7], [8], mf are postulated to provide desired motion signals, efference copy of motor commands, and error signals (desired trajectory - actual trajectory). These mf innervate Gr and Go. Go cells receive excitatory input from Gr cells while projecting back to Gr cells via inhibitory synapses, forming a negative feedback loop to regulate Gr activities. Gr cells axons called parallel fibers (pf) bifurcate and innervate both Ba/St cells and Pk cells via excitatory synapses. Ba/St cells project to Pk cells via inhibitory synapses, forming a negative feedforward pathway to Pk cells. Among these cells in the cerebellar cortex, Pk cells are the sole cell type that sends axon to extra-cerebellar regions. Pk cells receive another input

R. D. Pinzon-Morales and Y. Hirata are with Chubu University, Japan.  
yutaka@isc.chubu.ac.jp

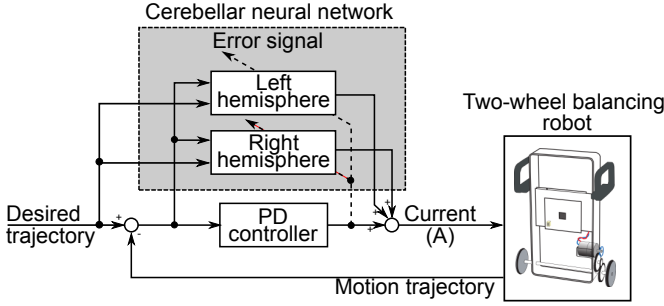


Fig. 1. The structure of the proposed controller rendering the bi-hemisphere cerebellar network (gray box) and the PD controller. Note that the PD output drives the adaptation in each hemisphere.

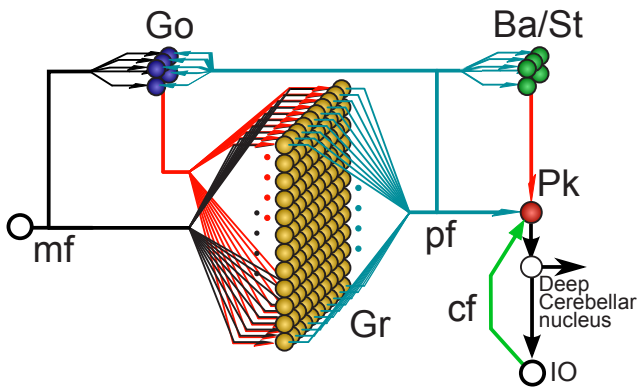


Fig. 2. Cerebellum microcircuit including granular (Gr) cells, Golgi (Go) cells, basket/stellate (Ba/St) cells, and Purkinje (Pk) cell, mossy fibers (mf), parallel fiber (pf), olfactory nucleus (IO), and climbing fibers (cf).

from inferior olivary nucleus (IO) via climbing fibers (cf) that is known to convey control error information. This cf input to Pk cells induces synaptic plasticity at Gr-Pk synapses. When Gr and cf are simultaneously active the efficacy of the synaptic transmission decreases (long-term depression : LTD), whereas when Gr alone is active the efficacy increases ( long-term potentiation: LTP). By these mechanisms, erroneous pf inputs (Gr activity) that caused control error are subject to be reduced while pf inputs that do not cause control error are enhanced. In this way, each Pk cell output is adjusted so that the control error is minimized [6].

The bi-hemispheric cerebellar neuronal network consists of two identical hemispheres each including 755 Gr, 5 Go, 5 Ba/St, 1 Pk cells. These numbers were the maximum possible with that the controller can run in real-time while preserving as close as possible to the actual ratio of the cell population and the convergence and divergence ratios of each cell type [9]. There are nine types of mf each of which carries the following signal: 1) desired body tilt angle (rad), 2) desired body tilt angular velocity (rad/s), 3) desired wheel angle (rad), 4) desired wheel angular velocity (rad/s), 5) body tilt angle control error (rad), 6) body tilt angular velocity control error (rad/s), 7) wheel angle control error (rad), 8) wheel tilt angular velocity control error (rad/s), 9) motor command efference copy. Each cell model is described as follows:

$$X_{Gr} = \sum_{mf=1}^7 W_{Grmf} \cdot Y_{mf} + \sum_{Go=1}^5 W_{GrGo} \cdot Y_{Go} \quad (1)$$

$$Y_{Gr} = \frac{2}{1 + e^{-X_{Gr}/\mu}} - 1 \quad (2)$$

$$X_{Go} = \sum_{mf=1}^7 W_{Gomf} \cdot Y_{mf} + \sum_{Gr=1}^{755} W_{GoGr} \cdot Y_{Gr} \quad (3)$$

$$Y_{Go} = \frac{2}{1 + e^{-X_{Go}/\mu}} - 1 \quad (4)$$

$$X_{Ba/St} = \sum_{Gr=1}^{755} W_{Ba/StGr} \cdot Y_{Gr} \quad (5)$$

$$Y_{Ba/St} = \frac{2}{1 + e^{-X_{Ba/St}/\mu}} - 1 \quad (6)$$

$$Y_{Pk} = \sum_{Gr=1}^{755} W_{PkGr} \cdot Y_{Gr} + \sum_{Ba/St=1}^5 W_{PkBa/St} \cdot Y_{Ba/St} \quad (7)$$

where  $Y_{\{\cdot\}}$  is the nonlinear output of each cell,  $W_{xy}$  represents the synaptic weight between cell  $x$  and cell  $y$ . Subscripts  $Gr$ ,  $Go$ ,  $mf$ ,  $Pk$ , and  $Ba/St$  are parameters for Gr, Go, mf, Pk, and Ba/St, respectively.

The proposed controller was implemented in LabVIEW 2010 (National Instrument, Austin, TX), running real time on a Windows laptop computer (4x2.40 Ghz Intel Core-i5 processor, memory: 3.8 GB), and communicating with the two-wheel robot (e-nuvo wheel, ZMP INC, Tokyo) via USART protocol at 57.6 Kbps.

#### B. Learning algorithm of the proposed controller

The learning rule governing the adaptability of the proposed controller follows the asymptotic Hebb rule, namely, the synaptic efficacies between Gr and Pk cells are updated according to the presence of control error signal conveyed by the cf activity (PD output) as follow:

$$\Delta W_{PkGr}(t) = \gamma_{LTD,LTP} \cdot Y_{Gr} \cdot (cf(t) - cf_{spont}) \quad (8)$$

$$W_{PkGr}(t+1) = W_{PkGr}(t) + \Delta W_{PkGr}(t) \quad (9)$$

where  $W_{PkGr}(t)$  is a synaptic weight between a Gr cell and a Pk cell at time  $t$ ,  $\gamma_{LTD,LTP}$  is the LTD and LTP learning rate, respectively;  $cf(t)$  is the climbing fiber input, and  $cf_{spont}$  is a DC level spontaneous activity of cf that has been shown to play an important role in bilateral motor control coordination in the cerebellum [10]. Using this learning algorithm with paired Gr and cf activity LTD occurs, whereas when only Gr activity is present LTP takes place. Learning rates  $\gamma_{LTD}$ ,  $\gamma_{LTP}$  were adjusted to be 0.001 and -0.005, respectively, which represent a trade off between learning speed and computational burden.

Left and right hemispheres, although they share the same structure, climbing fiber input is differentiate and split into left and right cf. Left hemisphere that governs the forward motion of the plant receives mainly forward error motion

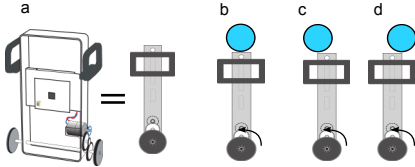


Fig. 3. Experimental protocol. a) front and lateral view of the two-wheel balancing robot. Two cases of perturbations (b-d) by adding an external load (blue circle). Forward motion (black arrow) is shown. b) balanced load placed on-centered. c) unbalanced load placed off-centered front. d) unbalanced load placed off-centered back.

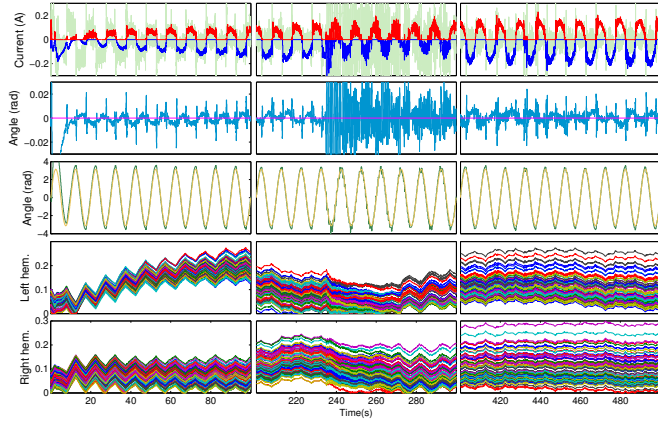


Fig. 4. Performance of the proposed controller with an external load placed on-centered of the robot at 235 s. From top first row: left hemisphere output (red), right hemisphere output (blue), PD output (green). Second row: body target tilt angle (magenta), body tilt angle actual position (light blue). Third row: wheel target angle position (yellow), wheel actual angle position (green). Third row: synaptic weights of the left hemisphere. Notice that columns shown different time windows: initial learning stage (left column), external load disturbance (middle column), and stabilization of the plant (right column).

signal, whereas the right hemisphere that governs the backward motion of the plant receives mainly backward error components. Although adaptation of each hemisphere is driven mainly by a preferred side motion error (forward error in the case of the left hemisphere), the  $cf_{spont}$  encodes non preferred side motion error (forward motion in case of the left hemisphere), such as that exhibit in the floccular Purkinje cell during vestibuloocular.

### III. RESULTS

#### A. Balanced load

When a 0.1 Hz sinusoidal trajectory was given as target motion for the wheel angle, and the body tilt angle was set to 0 deg, both the proposed controller and the PD controller alone were able to control the plant. However, when an external load (45% increase in mass) was placed on-centered of the robot (Fig. 3-b, referred as balanced load) the PD controller alone failed the control. In contrast, the proposed controller was able to handle this abrupt load change as shown in Fig. 4. During the first hundred seconds, before the load was imposed, the cerebellar controller proceeded learning and the output of each hemisphere gradually surpassed the

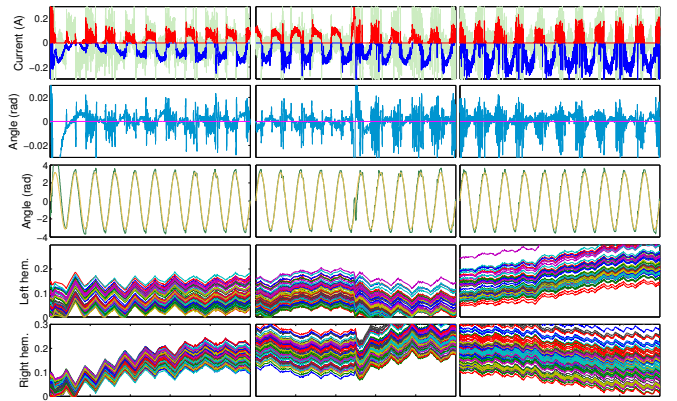


Fig. 5. Performance of the proposed controller with unbalanced load placed off-centered front of the robot at 250 s. Formats are the same as Fig. 4.

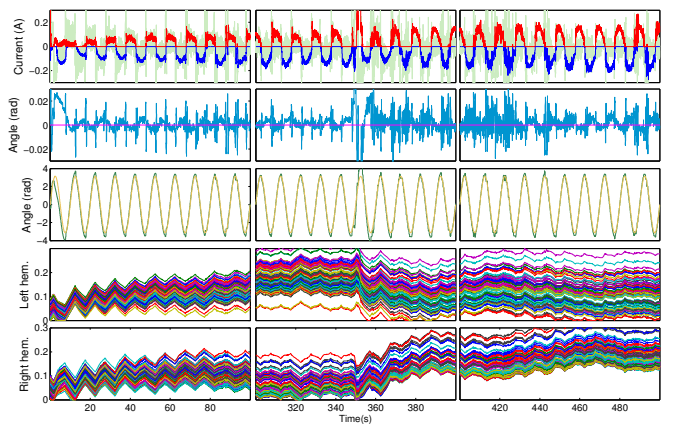


Fig. 6. Performance of the proposed controller with unbalanced load placed off-centered back of the robot at 350 s. Formats are the same as Fig. 4.

PD output. More interestingly, asymmetrical learning was observed between the two hemispheres, i.e., each hemisphere changed its weights differently to minimize the PD output. The greater weight changes of the left hemisphere may reflect the intrinsic asymmetry in the forward motion of the robot. When the external load was imposed, the immediate action against a novel error signal was the reduction of the Purkinje cell output due to LTD, which is reflected in the maintained decrease in the synaptic weights of both left and right hemispheres. After around 400 sec, the proposed controller became stabilized without major synaptic weight changes. This performance of the proposed controller is not surprising because we have demonstrated in our previous study that the single hemispheric cerebellar controller together with a PD controller was able to cope with a similar perturbation [3]. Thus, we tested the proposed controller in more challenging tasks that the single hemispheric controller would not be able to handle.

#### B. Unbalanced load

If the load is placed off-centered on the robot body to its front (Fig. 3-c) or to its back (Fig. 3-d) it causes a major dynamic asymmetry. We tested the proposed controller in

comparison with the previous single hemispheric controller in this task. As shown in Fig. 5 and Fig. 6, the proposed controller handled these load changes successfully. In contrast, neither the PD controller alone nor the single hemispheric controller could cope with this perturbation. It can be seen that in each case of the perturbation one of the hemispheres in charge of the motion that is affected by the perturbation exhibited larger output after a re-learning stage. When the load is off-centered to the front, the left hemisphere output (Fig. 5) presented the initial LTD followed by strong LTP so as to reduce the command error (PD output). On the other hand, the right hemisphere only presented short transient LTDs after the perturbation, and then only subtle LTPs were induced afterwards. When the load is added in the opposite side of the robot body (Fig. 6), the right hemisphere exhibited major changes.

#### IV. DISCUSSION

The bi-hemispheric cerebellar neural network controller configured in this study has an anatomically realistic architecture in terms of the ratios of the number of each cell type and synaptic connections, yet it can run in real-time for control of the two-wheel balancing robot. In our previous work, we demonstrated that a single hemisphere controller successfully controlled the two-wheel balancing robot after perturbations that symmetrically changed the load for forward and backward motions [3]. However, when asymmetrical loads were employed, this controller failed the control. One main reason for the failure of this configuration is that it cannot effectively compensate for the asymmetrical load changes. For example, adequate compensation for one direction to which more load change was imposed may cause overcompensation for the other direction. The proposed controller addressed such weakness of the previous controller by implementing a two-hemispheric structure of the cerebellum where forward and backward motion are distributed almost independently. The learning rule employed was also updated to be more realistic by carrying mainly unilateral error information [11]. Therefore, the left hemisphere in charge of the forward motion receives mainly forward motion error, and the right hemisphere receives mainly backward motion error.

In the future study, further testing of the performance of the proposed controller in more complex tasks, and comparison with conventional adaptive control methods will be carried out. A more realistic modeling of each neuron type using integrate-and-fire models [12] is also under construction. Additionally, the role of the inhibitory inter-neurons, Go cells and Ba/St cells will be investigated to understand the signal processing in the cerebellar cortical neuronal network during adaptive motor control.

#### REFERENCES

- [1] C. I. DeZeeuw, F. E. Hoebeek, L. W. J. Bosman, M. Schonewille, L. Witter, and S. K. Koekkoek, "Spatiotemporal firing patterns in the cerebellum," *Nature Reviews Neuroscience*, no. 12, pp. 327–344, June 2011.
- [2] A. J. Ijspeert, A. Crespi, D. Ryczko, and J.-M. Cabelguen, "From swimming to walking with a salamander robot driven by a spinal cord model," *Science*, vol. 315, no. 5817, pp. 1416–1420, 2007.
- [3] Y. Tanaka, Y. Ohata, T. Kawamoto, and Y. Hirata, "Adaptive control of 2-wheeled balancing robot by cerebellar neuronal network model," in *Engineering in Medicine and Biology Society (EMBC), 2010 Annual International Conference of the IEEE*, sept. 2010, pp. 1589 –1592.
- [4] A. Yoshikawa, M. Yoshida, and Y. Hirata, "Capacity of the horizontal vestibuloocular reflex motor learning in goldfish," in *Engineering in Medicine and Biology Society, 2004. EMBS '04. 26th Annual International Conference of the IEEE*, vol. 1, sept. 2004, pp. 478 –481.
- [5] B. Hu, X. Lin, L.-S. Huang, L. Yang, H. Feng, and J.-F. Sui, "Involvement of the ipsilateral and contralateral cerebellum in the acquisition of unilateral classical eyeblink conditioning in guinea pigs." *Acta Pharmacol Sin*, vol. 30, no. 2, pp. 141–52, 2009.
- [6] M. Ito, *The Cerebellum: Brain for an Implicit Self*, ser. FT Press Science. Pearson Education, 2011.
- [7] Y. Hirata and S. M. Highstein, "Acute adaptation of the vestibuloocular reflex: Signal processing by floccular and ventral parafloccular purkinje cells," *Journal of Neurophysiology*, vol. 85, no. 5, pp. 2267–2288, 2001.
- [8] P. M. Blazquez, Y. Hirata, S. A. Heiney, A. M. Green, and S. M. Highstein, "Cerebellar signatures of vestibulo-ocular reflex motor learning," *The Journal of Neuroscience*, vol. 23, no. 30, pp. 9742–9751, 2003.
- [9] S. Solinas, T. Nieuw, and E. D'Angelo, "A realistic large-scale model of the cerebellum granular layer predicts circuit spatio-temporal filtering properties," *Frontiers in Cellular Neuroscience*, vol. 4, no. 12, 2010.
- [10] R. Pinzon-Morales and Y. Hirata, "Bi-hemispheric model of the cerebellum with realistic climbing fiber input," in *Program No. 379.13. Soc. Neuroscience*, 2012.
- [11] Y. Hirata, P. M. Blazquez, K. Inagaki, K. Furuta, and S. M. Highstein, "Flocculus purkinje cell complex spikes during acute motor learning of the horizontal vestibuloocular reflex in squirrel monkeys," in *Program No. 805.6. Soc. Neuroscience*, 2006.
- [12] K. Inagaki, Y. Hirata, P. Blazquez, and S. Highstein, "Computer simulation of vestibuloocular reflex motor learning using a realistic cerebellar cortical neuronal network model," in *Neural Information Processing*, ser. Lecture Notes in Computer Science, M. Ishikawa, K. Doya, H. Miyamoto, and T. Yamakawa, Eds. Springer Berlin Heidelberg, 2008, vol. 4984, pp. 902–912.